Bull. Mater. Sci., Vol. 32, No. 4, August 2009, pp. 407–412. © Indian Academy of Sciences.

In situ templating synthesis of conic $Ba_{0.5}Sr_{0.5}Co_{0.8}Fe_{0.2}O_{3-\delta}$ perovskite at elevated temperature

WEI ZHOU, RAN RAN, ZONGPING SHAO* and WANQIN JIN

State Key Laboratory of Materials-Oriented Chemical Engineering, College of Chemistry and Chemical Engineering, Nanjing University of Technology, No. 5 Xin Mofan Road, Nanjing 210009, P.R. China

MS received 16 August 2008

Abstract. **Conic $Ba_{0.5}Sr_{0.5}Co_{0.8}Fe_{0.2}O_{3-\delta}$ (BSCF) functional composite oxide was synthesized via a simple *in situ* templating process. The treatment of the solid precursor with concentrated nitric acid resulted in the mismatch of ionic radius at *A*-site and *B*-site of the ABO_3 perovskite, due to the oxidation of cobalt/iron ions, and the formation of $Ba_{0.5}Sr_{0.5}(NO_3)_2$ solid solution. Therefore, instead of the direct formation of BSCF oxide, an intermediate phase of $Ba_{0.5}Sr_{0.5}CoO_3$ (BSC) in hexagonal lattice structure and with conic particle shape was preferentially formed during calcination at low temperature. BSCF perovskite was then produced by the *in situ* templating of BSC with iron diffusing into the BSC lattice during calcination at high temperature. Well-crystallized BSCF particles in conic shape were obtained by the calcination of the nitric acid treated precursor at 900°C.**

Keywords. **Perovskite; sol–gel; nitric acid; synthesis; EDTA–citric acid.**

1. Introduction

$Ba_{0.5}Sr_{0.5}Co_{0.8}Fe_{0.2}O_{3-\delta}$ (BSCF) is a perovskite-type composite oxide, which shows cubic structure at room and elevated temperatures (Koster and Mertins 2003). It possesses mixed oxygen ionic and electronic conductivity and variable oxygen nonstoichiometry in its structure at high temperature. Since first discovered by Shao *et al*, it has been recognized as a promising material for ceramic oxygen separation membrane and catalytic membrane reactor due to its outstanding oxygen permeability, high structural and chemical stabilities, together with the interesting catalytic activity for selective oxidation at high temperatures (Shao *et al* 2000, 2001a, b; Van Veen *et al* 2003; Liu and Gavalas 2005a, b; Chen *et al* 2007; Zeng *et al* 2007). More recently, it has also been recognized as a promising cathode material for intermediate temperature solid oxide fuel cells (SOFCs) due to its high surface oxygen exchange kinetics and bulk oxygen diffusion rate at reduced temperatures (Shao and Haile 2004; Shao *et al* 2005; Zhou *et al* 2007a,b, 2008a-d).

Tailoring the shape of a material on the micro- or nano-meter scale is one of the key problems. Normally, the shape of crystalline particles depends on their internal structure. This means that materials with a cubic structure will normally form isotropic particles, for example, cubes or octahedra. To modify the shape of particles with a cubic structure, it is necessary to apply special methods. In this study, we report the high-temperature synthesis of conic BSCF oxide via an indirect synthesis process, for the first time. By modifying the EDTA-citrate complexing process with the concentrated nitric acid treatment, an intermediate phase of $Ba_{0.5}Sr_{0.5}CoO_3$ (BSC) with hexagonal structure and conic morphology shape was formed during the calcination of the solid precursor at low temperature. The conic BSCF particles were obtained with the templating of the BSC phase at high temperature by the incorporation of iron into the BSC lattice.

2. Experimental

Analytical reagents of barium nitrate, $Ba(NO_3)_2$, strontium nitrate, $Sr(NO_3)_2$, cobalt nitrate, $Co(NO_3)_2{\cdot}xH_2O$, and iron nitrate, $Fe(NO_3)_3{\cdot}yH_2O$ were used as the starting materials for the synthesis of BSCF. The schematic diagram for the synthesis of BSCF is shown in figure 1. The metal nitrates were mixed into a solution according to the stoichiometric amounts. The necessary amount of EDTA–$NH_3{\cdot}H_2O$ and citric acid were then added to the solution. With the evaporation of water under stirring and heating, a transparent gel was obtained, which was then heated at 250°C for solidification. The obtained solid precursor was fired at high temperatures for the simultaneously burning out of the organic and the formation of the perovskite oxide. In some cases, the solid precursor was treated with a concentrated nitric acid before firing. In that case, necessary amount of concentrated nitric acid (67% wt.) was added to the solid precursor at room tempe-

*Author for correspondence (shaozp@njut.edu.cn)

rature. A vagarious exothermal reaction happened with a large amount of brown gas (NO_2) and white vapour (water) produced, due to the decomposition of HNO_3 as catalyzed by the metal ions and organics in the precursor. The reaction stopped after several minutes with the formation of a sticky gel or a foam-type solid precursor, depending on the amount of HNO_3 applied. The precursor was then further heat treated at 250°C for several hours, followed by firing at various temperatures.

Powder X-ray diffraction data were measured with a Bruker D8 Advance Diffractometer with CuKα radiation (λ = 1·5418 Å). Fourier transform infrared spectroscopy (FTIR, Thermo Nicolet Corporation AVATAR-360) of the precursors and calcined powders was recorded from 4000–400 cm^{-1} by the KBr pellet method. The morphologies and the energy dispersive X-ray (EDX) of the calcined powders were performed using a field emission scanning electron microscope (FE-SEM, LEO1530) equipped with energy dispersive spectrometer (EDS, INCA-300).

3. Results and discussion

EDTA–citrate combined complexing process is a simple and effective way to make metal ions mixed in the molecule level. We have successfully applied it for the synthesis of perovskite-type $La_{0.6}Sr_{0.4}Co_{0.2}Fe_{0.8}O_{3-\delta}$ (LSCF) composite oxide (Zhou *et al* 2006). With the help of EDTA and citric acid via chelating, metal ions La^{3+}, Sr^{2+}, Co^{2+}, and Fe^{3+} were mixed homogeneously within the precursor in molecular level, and nano-sized sphere-shape LSCF was synthesized by the calcination of the precursor at a temperature as low as 550°C. During the synthesis, no other phase except perovskite occurred. The sphere-shape particle configuration of the LSCF powder agreed well with the fact that LSCF took a quasi-cubic structure. It is normally believed that the geometric shape of the crystalline particles depends on their lattice structure. It means that materials with a cubic structure normally form isotropic particles, for example, spherical, cubic or octahedral particles (Wang and Li 2002).

The EDTA-citrate combined complexing process was also applied for the synthesis of BSCF in this study. The solid precursor then obtained was calcined at various temperatures for 5 h, and the corresponding XRD diffraction patterns are shown in figure 2. Different from the case of LSCF, some intermediate phases appeared before the formation of the perovskite oxide during the calcination process of the BSCF solid precursor. At a calcination temperature of 600°C for 5 h, X-ray diffraction patterns show the formation of $Ba_{1-x}Sr_xCO_3$ phase. The carbonate almost totally disappeared at the calcination temperature of 800°C, alongside with the appearance of some new phases in low intensity such as Co_3O_4, $BaFe_2O_{3-\delta}$, and $SrCoO_{3-\delta}$. A pure-phase BSCF was obtained at the calcination temperature of 900°C or higher. Figure 3 shows the SEM morphologies of BSCF powder calcined at 800°C and 900°C for 5 h, respectively. The sample calcined at 800°C displayed mainly of spherical granules with particle size of 80 to 150 nm, EDX results demonstrated that those particles are mainly composed of Ba, Sr, Co, Fe and O. However, small amount of conic particles were also observed with geometric size of ~1 μm in length and ~100 nm in bottom diameter. EDX results

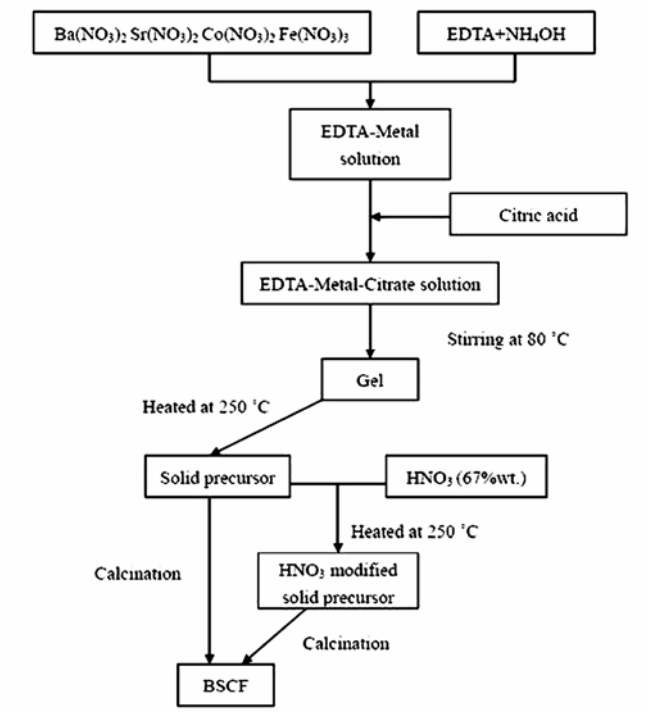

Figure 1. Schematic diagram for the preparation of conic BSCF powders by the *in situ* templating process.

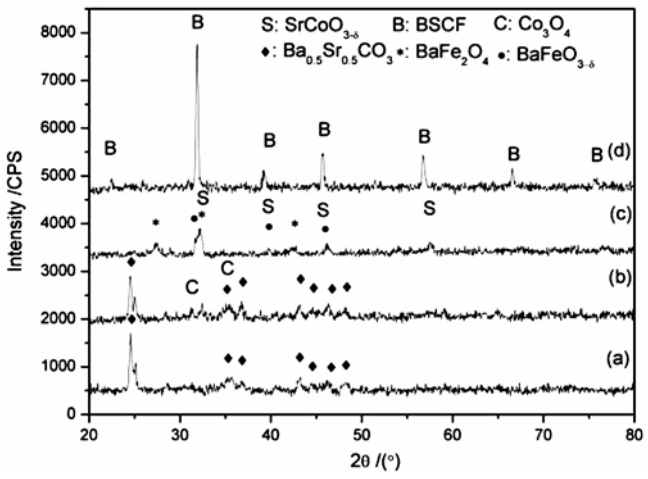

Figure 2. XRD patterns of the powders obtained by the calcination of BSCF solid precursor at various temperatures under air for 5 h, (a) 600°C, (b) 700°C, (c) 800°C and (d) 900°C.

show that those cones were composed of $Ba_{0.5}Sr_{0.5}CoO_3$ (BSC), however, due to the small amount of them, it was not detectable by powder X-ray diffraction. When the calcination temperature was further increased to 900°C, SEM results show that the obtained powder was mainly composed of spherical granules together with a small amount of conic particles. EDX results show that the needles had the same composition as that of the spherical granules, i.e. $Ba_{0.5}Sr_{0.5}Co_{0.8}Fe_{0.2}O_{3-\delta}$. Since BSCF displays a cubic perovskite structure, it is intrinsically difficult to synthesize BSCF in conic shape. It strongly suggests that the conic BSCF was synthesized in an indirect way. It was reported that $KNbO_3$ can be synthesized by the *in situ* templating of a $K_4Nb_6O_{17}$ intermediate phase (Pribošič *et al* 2005). It is likely that the conic BSCF was created based on the templating of conic BSC via the solid state diffusion of iron into the conic BSC lattice during calcination at 900°C. BSC is in hexagonal structure, it is intrinsically capable to form particles with special geometric shape, such as cone in this study. Although other intermediate phases such as $SrCoO_{3-\delta}$ could also be formed during the calcination, however, only BSC is in cone shape. It is then important that the intermediate phase of BSC should be maximized in order to prepare the conic BSCF in large scale.

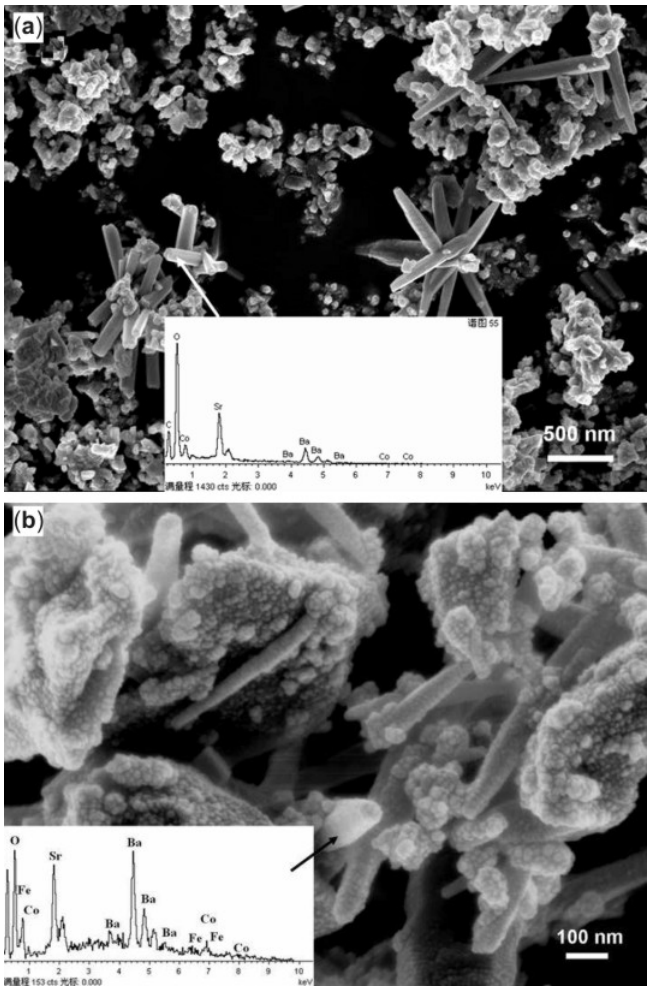

Figure 3. SEM images and EDTA profile for the samples obtained by the calcination of the solid precursor under air for (**a**) 800°C and (**b**) 900°C; the EDX profile indicates the composition of the cone in image.

For the preparation of composite oxide, the phase formation during the calcination process is closely related with the degree of the metal ions mixing in the precursor. When the metal ions are mixed homogeneously in the molecule level, the composite oxide with the most stable structure is preferentially formed during the calcination. The EDTA–citrate combined complexing process applies the chelating properties of EDTA and citric acid to immobilize the metal ions via the organic–metal ion legends. Figure 4 shows the conditional stability constants of Ba, Sr, Co, and Fe with EDTA. It indicates that Ba, Sr, Co and Fe can form stable complex with EDTA at pH > 6. With further contribution of citric acid as a secondly complexing agent, Ba^{2+}, Sr^{2+}, Co^{2+} and Fe^{3+} ions were mixed homogeneously in the molecule level, which is supported by the amorphous crystal structure of the solid precursor by X-ray diffraction patterns. The stoichiometry of the metal ions in the precursor was aimed for the formation $Ba_{0.5}Sr_{0.5}Co_{0.8}Fe_{0.2}O_{3-\delta}$ perovskite. However, the formation of perovskite is closely related with the Goldschmidt tolerance factor, defined as $t = (r_A + r_O)/\sqrt{2}(r_B + r_O)$, where r_A, r_B, and r_O are the ionic radius of metal ions A (12-coordinate), B (6-coordinate) and oxygen ions in ABO_3 structure, respectively. Perovskite structure can be formed only at t = 0·75–1. Once t is > 1·0 or < 0·75, the internal stress introduced from the mismatch of the radius of metal ions between A-site and B-site of perovskite was too large for the perovskite structure to survive. The tolerance factor of BSCF and LSCF is shown in figure 5. It is 1·02 for BSCF when cobalt and iron both took 3+ valence state. Although iron and cobalt

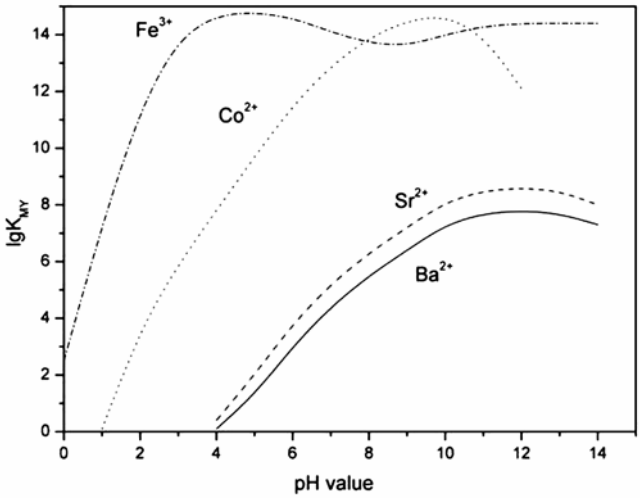

Figure 4. The pH value dependence of the conditional stability constants of EDTA-Ba, EDTA-Sr, EDTA-Co and EDTA-Fe complexes.

ions took 3+ ($Fe(NO_3)_3$) and 2+ ($Co(NO_3)_2$) valence states in the precursor, respectively, however, some of cobalt was oxidized to 3+ valence state during the calcination, as supported by the detection of the Co_3O_4 phase. During the calcination at low temperature, the solid-state diffusion was limited; therefore, the solid-state reaction was localized. In some micro-domains the cobalt and iron could both take 3+ valence state. BSCF perovskite could not be formed in those domains, because of the large internal stress originating from the mismatch of ionic radius at perovskite A-site and B-site. Therefore, intermediate phases were formed. With increasing calcination temperature, the cobalt and iron ions preferred to take lower valence state and the solid state diffusion became more significant. Once the valence states of cobalt and iron reached such values that the tolerance factor started to locate within the range of 0·75–1·0, BSCF perovskite was then formed. For the case of LSCF, t is always $< 1{\cdot}0$ whether cobalt took 3+ or 2+ valence state, it then well explained the fact that no intermediate phases appeared during the calcination process of LSCF precursor.

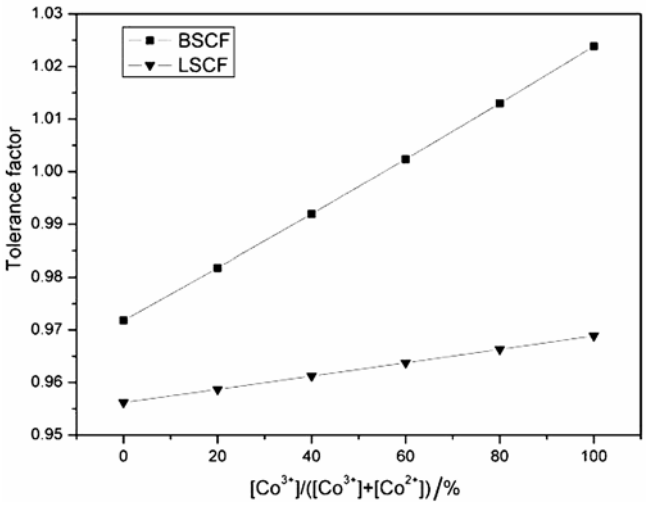

Figure 5. $[Co^{3+}]$ concentration dependence of the tolerance factors of BSCF and LSCF perovskites.

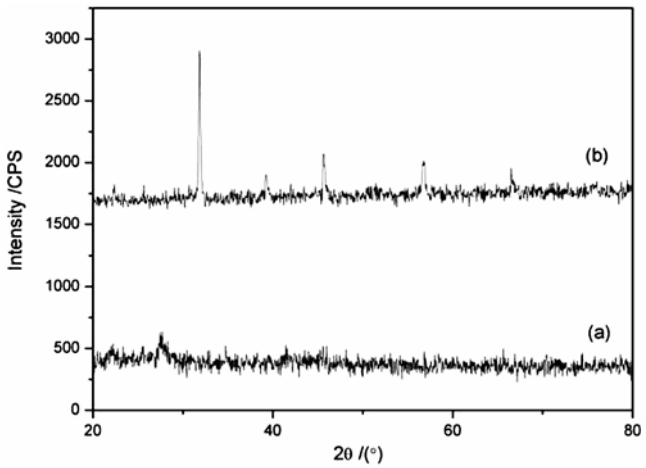

Figure 6. XRD patterns of the powders obtained by the calcination of BSCF solid precursor at (a) 800°C for 3 h under oxygen deficient condition, (b) the sample in (a) was further calcined at 900°C for 5 h under air.

In order to further testify that the formation of intermediate phases is closely related to the mismatch of ionic radius in perovskite, we calcined the BSCF precursor under oxygen deficient atmosphere at 800°C. This calcination led to the formation of carbon, which would react with cobalt and lead to the partial reduction of Co^{3+} to Co^{2+}. Therefore, the tolerance factor of BSCF successfully located within 0·75–1·0 ranges. X-ray diffraction results of the powders show that the formation of intermediate phases was indeed suppressed with no BSC or $SrCoO_{3-\delta}$ phases detected by XRD (figure 6). The SEM morphologies of the corresponding powders, as shown in figure 7, indicate that no any conic BSCF particle appeared in this case. It strongly supports our assumption that the conic BSCF was produced by the *in situ* templating of BSC.

Therefore, in order to prepare conic BSCF in large amount, it is important to increase the creation of cone-shaped BSC during the calcination. A novel process was then applied in this study. The solid precursor from EDTA–citrate combined complexing process was treated with concentrated nitric acid before firing. Figure 8 shows the X-ray diffraction patterns of BSCF solid precursors before and after nitric acid treatment. The initial solid precursor of BSCF indicated an amorphous structure. However, strong characteristic diffraction peaks of $Ba_{0{\cdot}5}Sr_{0{\cdot}5}(NO_3)_2$ (BSN) appeared after nitric acid treatment. Based on the results in figure 4, the conditional stability constant of Ba and Sr with EDTA are both less than zero at a pH value of < 4. It means that EDTA was

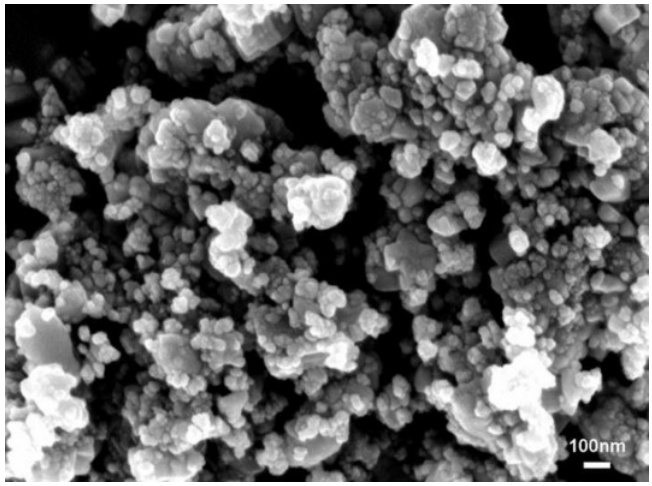

Figure 7. SEM morphology of BSCF powder obtained first by calcination of the solid precursor at 800°C under oxygen deficient condition for 3 h, followed by further calcination at 900°C under air for 5 h.

not able to immobilize Ba^{2+} and Sr^{2+} anymore under such condition. Therefore, the application of nitric acid treatment led to the break down of the ligands between EDTA/citric and Ba^{2+}/Sr^{2+}. The formation of BSN solid solution suggests that BSN phase is more stable than Ba/Sr complex under acid condition. The formation of BSN was further supported by the FTIR results as a strong adsorption peak appeared at 1386 cm^{-1} for the nitric acid treated sample, which is the characteristic N–O stretch vibration for NO_3^- (figure 9).

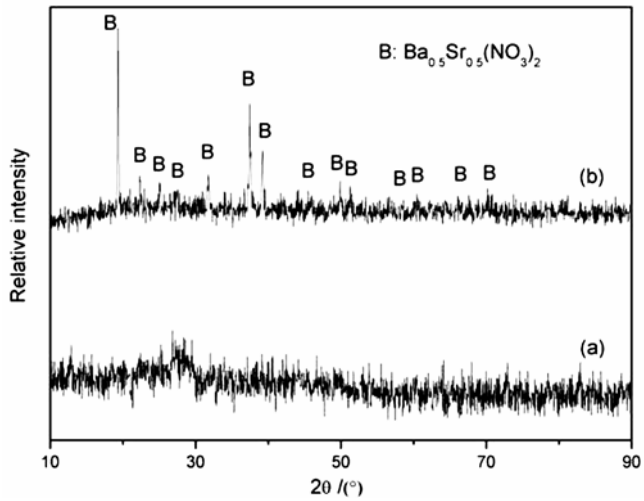

Figure 8. XRD patterns of BSCF solid precursor (a) before nitric acid treatment and (b) after nitric acid treatment.

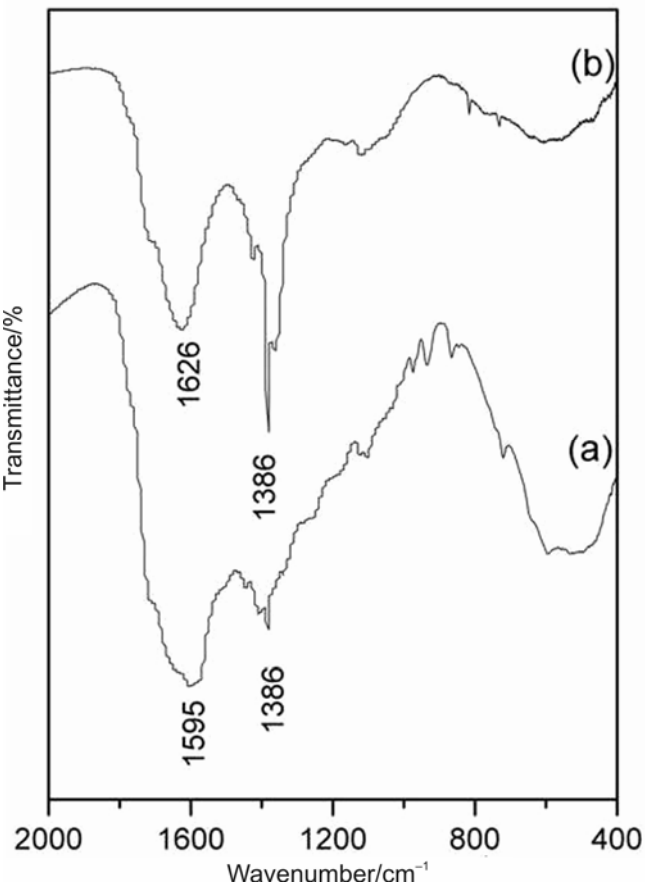

Figure 9. FT–IR spectra of the BSCF solid precursor (a) before nitric acid treatment and (b) after nitric acid treatment.

The nitric acid treated samples were then calcined at various temperatures for 5 h. The X-ray diffraction patterns of the resulted samples are shown in figure 10. At a calcination temperature of 600°C, the main detectable phase by XRD was $Ba_{1-x}Sr_xCO_3$, suggesting the formation of carbonate. However, at a calcination temperature of 700°C, the strongest diffraction peaks were that of BSC, while $SrCoO_{3-\delta}$ phase was in much lower intensity. When the calcination temperature increased to 900°C, the pure-phase BSCF perovskite was totally formed. Based on above results, it suggests that BSCF was mainly formed via an indirect process by the *in situ* template of BSC. Figure 11 shows the SEM–EDX results of the samples from the calcination of the nitric acid treated precursor at 800 and 900°C for 5 h, respectively. The conic particles were indeed detected after the calcination at 800°C for 5 h, with the increase of calcination temperature to 900°C, the powder was mainly in conic shape with 2 ~ 3 μm in length and 100 ~ 200 nm in bottom diameter, the EDX results show that the cones have the aimed composition of BSCF.

Based on above results, it suggests that the nitric acid treatment of solid precursor from combined EDTA–citrate process led to the preferential formation of intermediate phase of conic BSC during calcination. The role of HNO_3 treatment in obtained conic BSCF could be double. Firstly, HNO_3 is a strong oxidant, it oxidized cobalt and iron ions in the precursor to higher valence states during treatment and calcination, therefore, the ionic radius mismatch at A-site and B-site of BSCF was exaggerated.

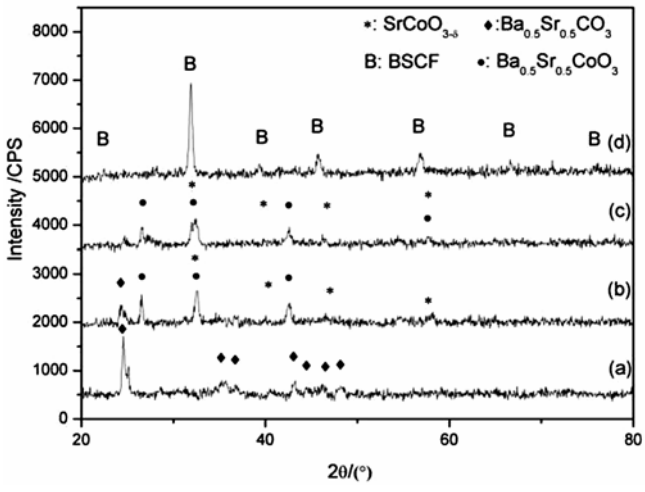

Figure 10. XRD patterns of the powders obtained by calcination of the BSCF solid precursor at various temperatures under air for 5 h (a) 600°C, (b) 700°C, (c) 800°C and (d) 900°C.

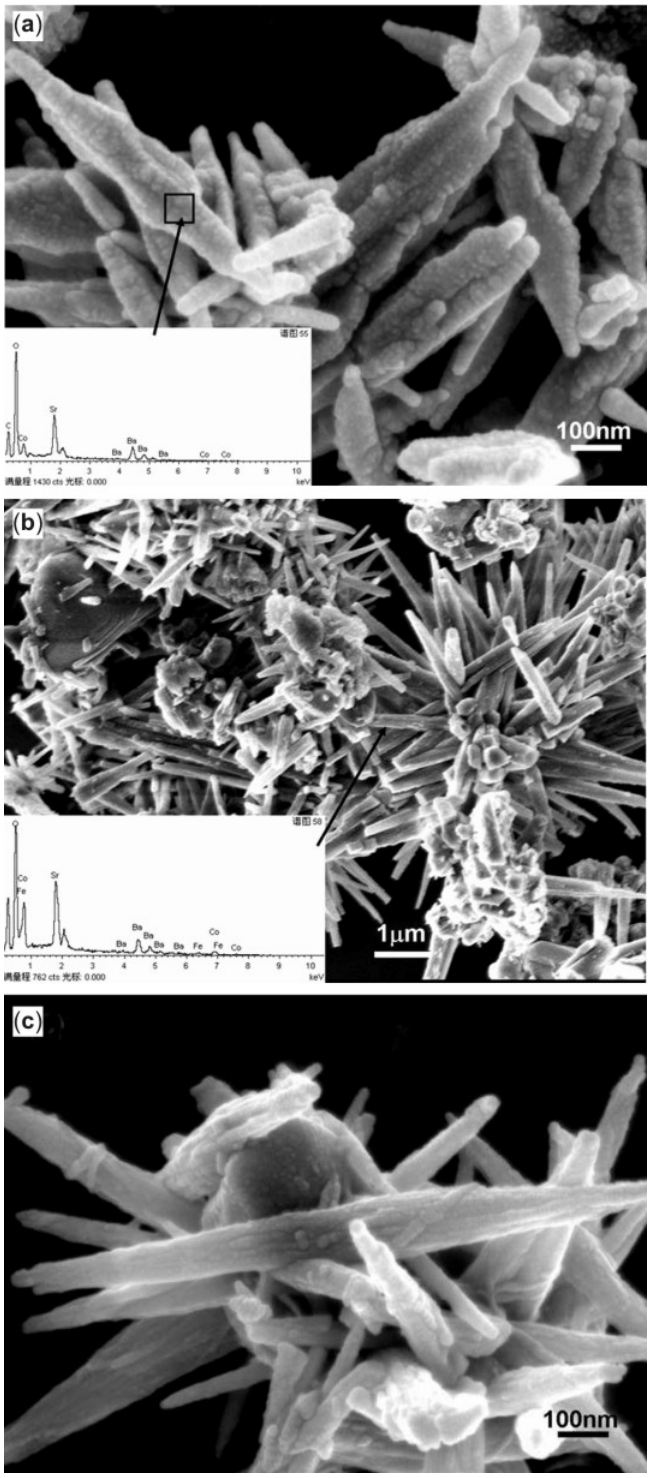

Figure 11. SEM images and EDX profiles of the samples obtained by calcination of the nitric acid treated BSCF solid precursor at various temperatures for 5 h in air (**a**) 800°C, (**b**) 900°C and (**c**) magnification of cones in (**b**).

Furthermore, the HNO_3 treatment of the solid precursor led to the formation of BSN solid solution, as shown in figures 8 and 9, which helped to form the BSC and suppress the $SrCoO_{3-\delta}$.

4. Conclusions

The conic BSCF particles were synthesized at high-temperature via an indirect synthesis process for the first time. By modifying the EDTA–citrate complexing process with treatment by concentrated nitric acid, an intermediate phase of BSC with hexagonal structure and conic shape was preferentially formed during the calcination of the solid precursor at low temperature. The as-produced BSC was then served as a template for the synthesis of conic BSCF via the iron ion diffusing into the lattice.

Acknowledgements

This work was supported by the National Natural Science Foundation of China under contract Nos. 20646002, and 20676061, by the National 863 program under contract No. 2007AA05Z133, and by the National Basic Research Program of China under contract No. 2007CB209704.

References

Chen Z H, Ran R, Zhou W, Shao Z P and Liu S M 2007 *Electrochim. Acta* **52** 7343
Koster H and Mertins F H B 2003 *Powder Diffr.* **18** 56
Liu S M and Gavalas G R 2005a *J. Membr. Sci.* **146** 103
Liu S M and Gavalas G R 2005b *Ind. Eng. Chem. Res.* **44** 7633
Pribošič I, Makovec D and Drofenik M 2005 *Chem. Mater.* **17** 2953
Shao Z P, Yang W S, Cong Y, Dong H, Tong J H and Xiong G X 2000 *J. Membr. Sci.* **172** 177
Shao Z P, Xiong G X, Tong J H, Dong H and Yang W S 2001a *Sep. Purif. Technol.* **25** 97, 420
Shao Z P, Dong H, Xiong G X, Cong Y and Yang W S 2001b *J. Membr. Sci.* **183** 181
Shao Z P and Haile S M 2004 *Nature* **431** 170
Shao Z P, Haile S M, Ahn J, Ronney P D, Zhan Z L and Barnett S A 2005 *Nature* **435** 795
Van Veen A C, Rebeilleau M, Farrusseng D and Mirodatos C 2003 *Chem. Commun.* **1** 32
Wang X and Li Y 2002 *J. Am. Chem. Soc.* **124** 2880
Zeng P Y, Chen Z H, Zhou W, Gu H X, Shao Z P and Liu S M 2007 *J. Membr. Sci.* **291** 148
Zhou W, Shao Z P and Jin W Q 2006 *J. Alloy Compds.* **426** 368
Zhou W, Shao Z P, Ran R, Chen Z H, Zeng P Y, Gu H X, Jin W Q and Xu N P 2007a *Electrochim. Acta* **52** 6297
Zhou W, Shao Z P, Ran R, Zeng P Y, Gu H X, Jin W Q and Xu N P 2007b *J. Power Sources* **168** 330
Zhou W, Ran R, Shao Z P, Gu H X, Jin W Q and Xu N P 2008a *J. Power Sources* **174** 237
Zhou W, Ran R, Shao Z P, Zhuang W, Jia J, Gu H X, Jin W Q and Xu N P 2008b *Acta Mater.* **56** 2687
Zhou W, Ran R, Shao Z P, Jin W Q and Xu N P 2008c *J. Power Sources* **182** 24
Zhou W, Ran R, Shao Z P, Cai R, Jin W Q, Xu N P and Ahn J 2008d *Electrochim. Acta* **53** 4370